ELSEVIER

Biochimica et Biophysica Acta 1417 (1999) 183–190

BIOCHIMICA ET BIOPHYSICA ACTA
BBA

Rapid report

An ordered metastable phase in hydrated phosphatidylethanolamine: the Y-transition

Boris Tenchov [a,*], Rumiana Koynova [a], Michael Rappolt [1,b], Gert Rapp [b]

[a] *Institute of Biophysics, Bulgarian Academy of Sciences, Acad. G. Bonchev str. 21, 1113 Sofia, Bulgaria*
[b] *European Molecular Biology Laboratory, Outstation at DESY, D-22603 Hamburg, Germany*

Received 14 December 1998; accepted 22 December 1998

Abstract

By using time-resolved X-ray diffraction, differential scanning calorimetry and scanning densitometry, we observed rapid formation at low temperature of a metastable ordered phase, termed L_{R1} phase, in fully hydrated dihexadecylphosphatidylethanolamine (DHPE). The L_{R1} phase has the same lamellar repeat period as the gel L_β phase but differs from the latter in its more ordered, orthorhombic hydrocarbon chain arrangement. It forms at about 12°C upon cooling and manifests itself as splitting of the sharp, symmetric wide-angle X-ray peak of the DHPE gel phase into two reflections. This transition, designated the 'Y-transition', is readily reversible and proceeds with almost no hysteresis between cooling and heating scans. Calorimetrically, the $L_{R1} \rightarrow L_\beta$ transition is recorded as a low-enthalpy (0.2 kcal/mol) endothermic event. The formation of the L_{R1} phase from the gel phase is associated with a small, about 2 μl/g, decrease of the lipid partial specific volume recorded by scanning densitometry, in agreement with a volume calculation based on the X-ray data. The formation of the equilibrium L_c phase was found to take place from within the L_{R1} phase. This appears to be the only observable pathway for crystallisation of DHPE upon low-temperature incubation. Once formed, the L_c phase of this lipid converts directly into L_β phase at 50°C, skipping the L_{R1} phase. Thus, the L_{R1} phase of DHPE can only be entered by cooling of the gel L_β phase. The data disclose certain similarities between the low-temperature polymorphism of DHPE and that of long-chain normal alkanes.

Keywords: Lipid membrane; Lipid polymorphism; Phase transition; Metastability; Subgel phase; Differential scanning calorimetry; Densitometry; X-ray diffraction

When subjected to low temperatures, the lamellar phases formed by stacks of lipid bilayers are known to revert from their fluid, liquid crystalline state into a variety of crystalline and gel phases [1]. Except as a contribution to a better understanding and characterisation of the lipid phase behaviour, the studies on the low-temperature lipid phases have relevance to various other issues. Such studies provide the physical means to interpret the biomembrane response to extreme conditions – low temperatures, freezing of water, and related dehydration. The fluid-to-solid transitions strongly affect the lipid mixing behaviour

Abbreviations: PE, phosphatidylethanolamine; DHPE, dihexadecyl PE; PC, phosphatidylcholine; DPPC, dipalmitoyl PC; DSC, differential scanning calorimetry; TRXRD, time-resolved X-ray diffraction; SAX, small-angle X-ray diffraction; WAX, wide-angle X-ray diffraction

* Corresponding author. Fax: +359-2-971-2493; E-mail: tenchov@obzor.bio21.bas.bg

[1] Present address: Sinhrotrone Trieste, Bassovizza, 34012 Trieste, Italy.

0005-2736/99/$ – see front matter
PII: S0005-2736(98)00259-4

and the properties of the lipid–protein complexes as well. They also modulate the vesicle adsorption to interfaces, including cellular surfaces.

In the present work we investigate the low-temperature phase behaviour of fully hydrated dihexadecylphosphatidylethanolamine (DHPE). This phospholipid is widely explored in model studies, partly because of its ability to form both lamellar and non-lamellar phases in accessible temperature range. Dispersions of DHPE in excess water display reversible lamellar gel (L_β)–lamellar liquid crystalline (L_α)–inverted hexagonal (H_{II}) phase transitions at about 69°C and 85°C, respectively [1]. Upon prolonged equilibration at low temperature, a crystalline (subgel) L_c phase forms as well [2]. Since, upon heating, the L_c phase of DHPE converts endothermically into L_β phase at about 50°C (a subtransition), the L_β phase should be therefore considered metastable at lower temperatures and subject to spontaneous relaxation into L_c phase. Here we demonstrate that aqueous DHPE dispersions also form another ordered solid phase, designated L_{R1} phase, at temperatures below 12°C, which does not require low-temperature incubation but constitutes immediately upon cooling of the gel phase. This phase is deemed important as it appears to mediate the conversion of the gel L_β phase of DHPE into L_c phase. The existence of similar ordered phases in hydrated PEs (distearoyl PE, ditetradecyl PE) as well as in phosphatidic acids dispersed in 1 M NaCl solution has been noticed previously [3,4]. Transitions with similar symptoms, between the L_β' phase and an ordered metastable low-temperature phase SGII, have been documented to take place also in DPPC and other saturated diacyl PCs [5–7]. This report provides a structural and thermodynamic characterisation of the reversible transition between the L_β and L_{R1} phases of DHPE by means of time-resolved X-ray diffraction, differential scanning calorimetry and scanning densitometry. The data disclose a certain correspondence between the low-temperature behaviour of hydrated DHPE and the thermotropic polymorphism of long-chain normal alkanes.

DHPE (1,2-dihexadecyl-*sn*-glycero-3-phosphoethanolamine) from Fluka, Basel, Switzerland (>99% pure) was used without further purification. The lipid was found to migrate as single spot in thin-layer chromatography checks. Microcalorimetric scans of its diluted dispersion showed highly cooperative chain melting phase transition ($\Delta T_{1/2} < 0.4$°C), at temperature in agreement with the published values thus providing another guarantee that the lipid purity corresponds to the claimed one of 99%. Doubly distilled deionised water was added to weighed amounts of lipid. The dispersions were hydrated overnight at 20°C and cycled 8–10 times between about 75°C and an ice bath. The samples were vortex-mixed at these temperatures for 1–2 min at each cycle. The lipid concentrations were 5–10 mg/ml for calorimetry, 20–30 mg/ml for densitometry and 20–45 wt.% for TRXRD. For TRXRD measurements, samples were sealed into glass capillaries, or into flat cells with mica windows. Samples prepared at low temperature ('cold' samples) were also used. These samples were homogenised by 5–10 successive cycles of freezing at −18°C, followed by thawing at temperature below 10°C and vortexing during the thawing step.

X-Ray diffraction patterns were recorded at beam line X13 of EMBL at DESY, Hamburg. A brass sample holder was connected to a temperature control system as described recently [8]. The camera comprises a double focusing monochromator–mirror arrangement [9]. X-ray reflections in the small- and wide-angle regimes were recorded simultaneously using a data-acquisition system previously described [10]. Typical resolutions were 1/(180 nm) for the WAX range, and from 1/(620 nm) to 1/(1000 nm) for the SAX range. The calibration standards used were verified against a silicon standard. Raw data were normalised for the incident beam intensity. No further corrections were applied. No radiation damage of the lipids was evident from their X-ray patterns. Some samples with longer exposure time were checked by thin layer chromatography after the experiments. However, no products of lipid degradation were detected in these samples. The data were analysed using the interactive data evaluating program OTOKO [11].

Microcalorimetric measurements were performed using high-sensitivity differential adiabatic scanning microcalorimeters DASM-1M and DASM-4 (Biopribor, Pushchino, Russia). Heating runs at scan rate of 0.5°C/min were followed by passive cooling in the calorimetric cell. Cooling from 20°C to 0°C together with the equilibration for the subsequent heating

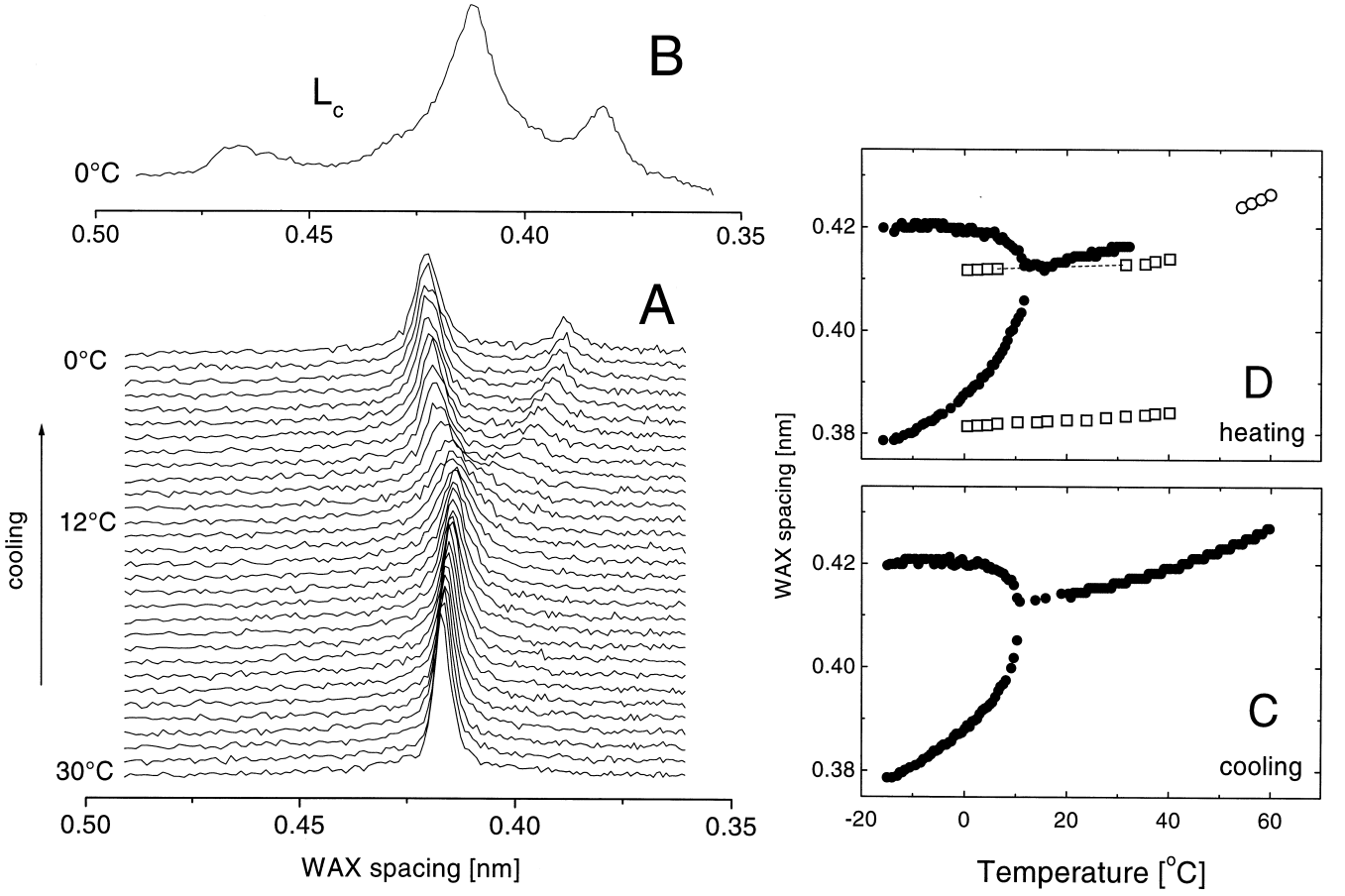

Fig. 1. Splitting of the wide-angle reflection of the gel phase of DHPE dispersions (the Y-transition). (A) Diffraction patterns recorded at cooling rate 1°C/min. Data were recorded for 2 s every 30 s. Every second frame is shown in the figure; (B) diffraction pattern of an L_c phase in unheated DHPE dispersion ('cold' preparation); (C) WAX spacings upon cooling (scan rate 0.1°C/min at $T<20$°C); (D) WAX spacings upon heating at 0.1°C/min (black circles). The open squares represent the two prominent reflections of the L_c phase, and the open circles the gel phase obtained through an $L_c \rightarrow L_\beta$ transition.

scan typically took about 1–1.5 h. Transition enthalpies and temperatures were determined in a standard way, as previously described [2].

The specific volume of the lipid molecules as a function of temperature was calculated from the density difference between water and the lipid dispersions. This difference was recorded with two DMA 602H cells (Anton Paar, Graz, Austria) connected to a home-built unit for data acquisition and temperature control. Linear heating and cooling scans of the samples were performed at 0.1–1.0°C/min with a PC-interfaced water bath. The instrument constants were determined according to the specifications of the producer, using distilled water and air as standards. The densities of air and water as a function of temperature were taken from the CRC Handbook of Chemistry and Physics [12]. The partial specific volume $\bar{\nu}$ of lipid was calculated as

$$\bar{\nu} = \frac{1}{\rho_2}\left(1-\frac{\rho_1-\rho_2}{c}\right),$$

where ρ_1 and ρ_2 are the densities of the lipid dispersion and water, respectively, and c is the lipid concentration.

When cooled from the liquid crystalline L_α phase, hydrated DHPE forms lamellar gel L_β phase, with lamellar repeat distance of 6.08 nm and sharp, symmetric WAX reflection at 0.427 nm at 60°C, characteristic for a hexagonal chain arrangement. The shape of the WAX reflection indicates that the DHPE chains are parallel to the bilayer normal [13], as appears to be typical for the PE gel phases

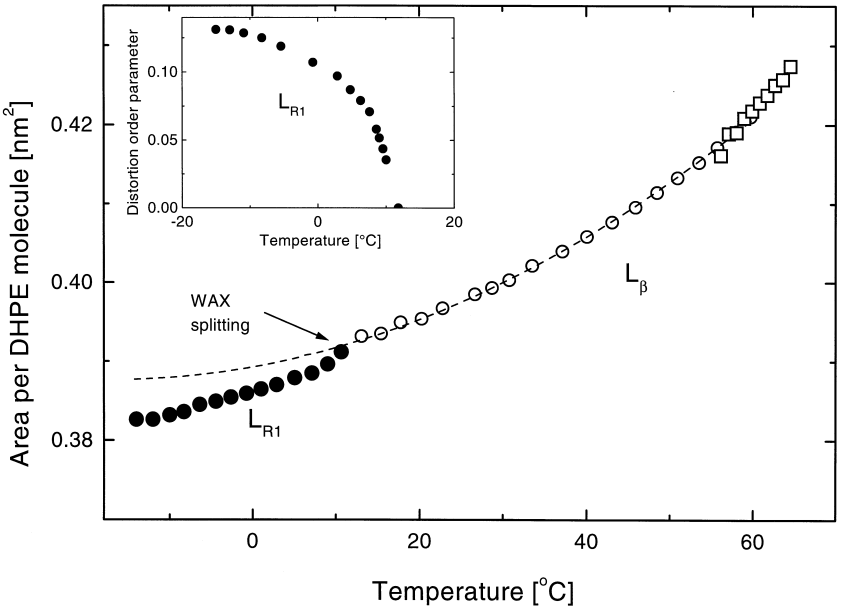

Fig. 2. Surface area of a DHPE molecule calculated from the wide-angle X-ray data. Circles, cooling scan from L_α phase; squares, first heating scan of a 'cold' sample undergoing $L_c \rightarrow L_\beta$ transition at 50°C (Fig. 1D). Open symbols refer to the L_β phase; closed symbols refer to the L_{R1} phase. The dashed line is the best fit ($S = 5.611 \times 10^{-6} T^2 + 1.889 \times 10^{-4} T + 0.3892$) to the L_β surface area per DHPE molecule. The inset shows the distortion order parameter (see text for details).

[14]. Further cooling produces gradual shrinking of the hydrocarbon chain lattice, as visualised by the decrease of the WAX spacing to 0.414 nm at 20°C and 0.413 nm at 13°C (Fig. 1). This process is interrupted by splitting of the WAX peak into two reflections at about 12°C, signalling the transition of the gel phase into another phase which we denote as L_{R1} phase. Lowering the temperature results in continuous further separation of the two wide-angle peaks to spacings of 0.379 nm and 0.420 nm at −15°C. The water freezing in these samples takes place at about −17°C, as determined by cooling scans to −25°C. It is evidenced by the appearance of ice peaks in the WAX pattern, coinciding with sharp release of heat (data not shown). The positions of the WAX spacings of the L_{R1} phase given in Fig. 1C,D did not change upon several hours of incubation at several temperatures below 12°C (6, 3, 0, −3 and −15°C). We therefore consider the peak separation as a temperature-dependent characteristic of this phase, not influenced by the kinetics of the $L_\beta \rightarrow L_{R1}$ transformation. This splitting, which we earlier reported for DHPE dispersions in 0.5–2.4 M sucrose solutions and designated the 'Y-transition' [15], is accompanied by no change in the lamellar repeat distance. The latter slightly expands initially, from 6.08 nm to 6.21 nm in the temperature range 60–25°C, and remains further unchanged, at least in the range from 25°C to 0°C. The constancy of the lamellar spacing provides a reasonable guarantee that the lipid chains remain parallel to the bilayer normal during the $L_\beta \rightarrow L_{R1}$ transition. As could be seen from Fig. 1, the transition proceeds first as broadening of the gel peak, followed by separation of the higher-angle peak which shifts away at a higher rate than the lower-angle peak. The Y-transition is fully reversible with very small or no hysteresis (Fig. 1C,D). It is perfectly reproducible and weakly dependent on the scan rate in the explored range 0.1–1°C/min.

The splitting of the single WAX band characteristic for the gel phase into a strong band at 0.420 nm and a weaker band at 0.379 nm indicates a distortion of the hydrocarbon chain arrangement from hexagonal packing, with $d_{110} = d_{\bar{1}10} = d_{200} = 0.414$ nm at 20°C, into an orthorhombic packing with $d_{110} = d_{\bar{1}10} = 0.420$ nm and $d_{200} = 0.379$ nm at −15°C. The extent of distortion with the temperature may be quantified by introducing a distortion order parameter, $\mathbf{D = 1 - a/b\sqrt{3}}$, where $\mathbf{a = 2d_{200}}$ and $\mathbf{b = 2d_{200}\ \tan(\arcsin(d_{110}/2d_{200}))}$ (Fig. 2, inset). By def-

inition, $\mathbf{D}=0$ in the L_β phase. At low temperature the order parameter increases up to $\mathbf{D}=0.132\pm0.02$, approaching a limiting ratio $\mathbf{a/b}=1.5$. The surface area per lipid molecule is given by $\mathbf{S}=\mathbf{a.b}$. It is 0.396 nm^2 for the hexagonal chain arrangement at 20°C, and 0.382 nm^2 for the orthorhombic one at −15°C. Its temperature dependence, as determined from a cooling scan, is given in Fig. 2. At temperatures below 12°C the surface area declines from the extrapolated trendline followed for the gel phase at higher temperatures. However, the L_{R1} lipid area of 0.382 nm^2 at −15°C (0.191 nm^2 per chain) is still higher than the most compact packings attainable by double-chained lipids, typified by the doubled value for the minimum area per chain of normal alkanes, $S=0.180$–0.185 nm^2, in their crystalline orthorhombic form [16,17]. Also, the L_{R1} phase lamellar spacing is significantly higher than the L_c phase lamellar spacing of $d=5.60$ nm, measured with DHPE 'cold' samples, at least partially due to the higher lipid hydration in the former state.

A cross-sectional area decline taking place at constant lamellar period suggests that the lipid volume decreases during the $L_\beta \rightarrow L_{R1}$ transition. This effect was clearly displayed by scanning densitometry. As is seen in Fig. 3A, in the range from 12°C to 0°C the DHPE specific volume declines by 2 μl/g from the extrapolated temperature dependence of the gel phase specific volume. This decrease is reversible without prominent hysteresis and is reproducibly observable at any tested scan rate in the range 0.1–1°C/min.

Using the densitometrically measured partial specific volumes, the areas per DHPE molecule given in Fig. 2, and the lamellar repeat distance, one may evaluate various parameters of the hydrated lipid bilayers. For the limiting hydration of the DHPE gel phase at 20°C we obtain a value of 14.5 w% (6.3 H_2O molecules per DHPE). This value is within the range of 6–6.5 H_2O molecules given by Seddon et al. [18], and is lower than those of 16–20 w% given by Caffrey [19], and 18.7 w% given by Hing et al. [20]. The increment per CH_2 group of the DHPE hydrocarbon chains can be estimated as follows. The partial specific volume of 0.946 ml/g at 20°C (cf. Fig. 3A) corresponds to a DHPE molecular volume of 1.043 nm^3. The latter is the sum of the head group and hydrocarbon chain volumes. For the volume of the DHPE head group (including the glycerol backbone) we use the value 0.252 nm^3 determined by Nagle and Wiener for fully hydrated dilauroyl PE in gel state [21]. In such way we obtain an increment of 0.125 nm per CH_2 group, showing that the DHPE hydrocarbon chains are almost fully stretched at 20°C. Indeed, from a backward calculation, using an increment of 0.127 nm per CH_2 group (the standard value for crystalline paraffins in all-trans chain conformation), we obtain a partial specific volume of 0.958 ml/g, which is only slightly above the densitometrically measured one.

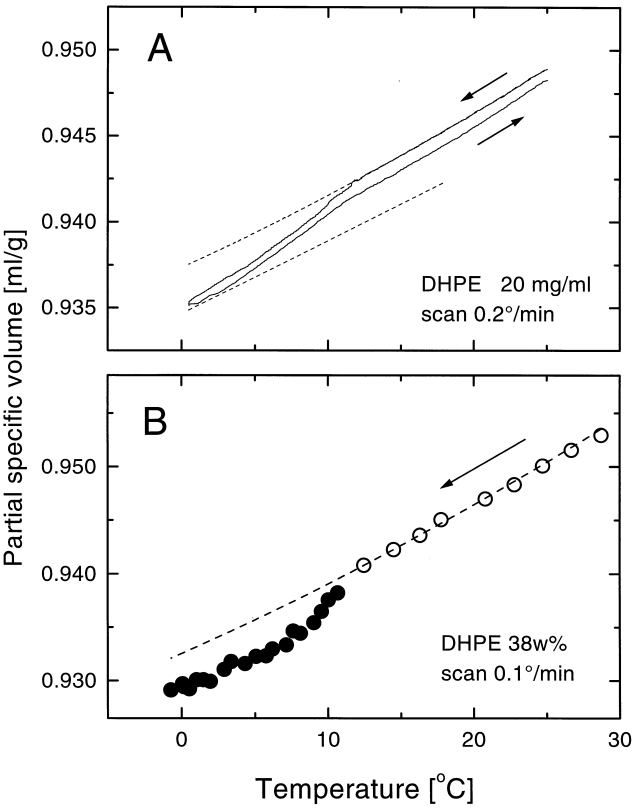

Fig. 3. Partial specific volume of DHPE dispersed in excess water. (A) Determined by differential scanning densitometry; (B) calculated from the X-ray data (details are given in the text).

Further, in order to calculate the specific volume of the L_{R1} phase from the X-ray data alone, we assume that the volume of the DHPE head group does not change during the $L_\beta \leftrightarrow L_{R1}$ transition. This assumption appears reasonable, once the lamellar repeat distance remains unchanged, and the mean cross section of a PE head group (about 0.33 nm^2)

remains always smaller than the cross-section of the two hydrocarbon chains. In this way we attribute the volume decrease, associated with the L_{R1} formation, entirely to the DHPE area decline shown in Fig. 2. The partial specific volume of the L_{R1} phase of DHPE, calculated with CH_2 increment of 0.125 nm, is given in Fig. 3B. It is 0.929 ml/g at 1°C, rather close (within 1%) to the densitometric value. A complete match between calculated and measured specific volumes of DHPE can be obtained if we assume an increase of the CH_2 increment from 0.125 nm at 20°C to 0.126 nm at 1°C. At the latter temperature, the difference between the extrapolated L_β volume and the L_{R1} volume of DHPE is 1.8 μl/g (Fig. 3B), very similar to the volume change determined by densitometry (Fig. 3A). Thus, at all temperatures in the measured range the DHPE partial specific volumes calculated from the structural data closely agree with the densitometric values, and both data sets consistently show that a small, reversible volume decrease of about 2 μl/g accompanies the formation of the L_{R1} phase.

Dispersion of DHPE in excess water displays $L_\beta \rightarrow L_\alpha$ transition at 68.9°C and $L_\alpha \rightarrow H_{II}$ transition at 85.6°C (Fig. 4, inset), in agreement with published data (for a survey, see [1,22]). Upon first heating after low-temperature sample preparation or after prolonged incubation at low temperature, it displays also an $L_c \rightarrow L_\beta$ transition at 50°C, with an enthalpy of 6.3 kcal/mol (Fig. 4). Cooling to 0°C and immediate reheating do not restore the transition at 50°C. Instead, an anomaly in the excess heat capacity curve is observed around 10°C, with area corresponding to 0.22 kcal/mol. The latter peak is completely reproducible in immediate subsequent scans. Incubation for up to 60 h at 3°C does not change noticeably its temperature and area. After 60 h incubation, however, initial traces of the transition at 50°C may also appear on the thermogram (Fig. 4). The equilibration time required for reappearance of the $L_c \rightarrow L_\beta$ transition is rather sensitive to the particular temperature protocol. As is seen from Fig. 4, cooling to −18°C for 30 min, followed by storage at 3°C, may considerably accelerate the recovery of the $L_c \rightarrow L_\beta$ transition – about 10% of the lipid has been observed to be converted into L_c phase after 3 h, while after 15 h it is already 40–50%, as estimated from the area of the $L_c \rightarrow L_\beta$ peak. During this

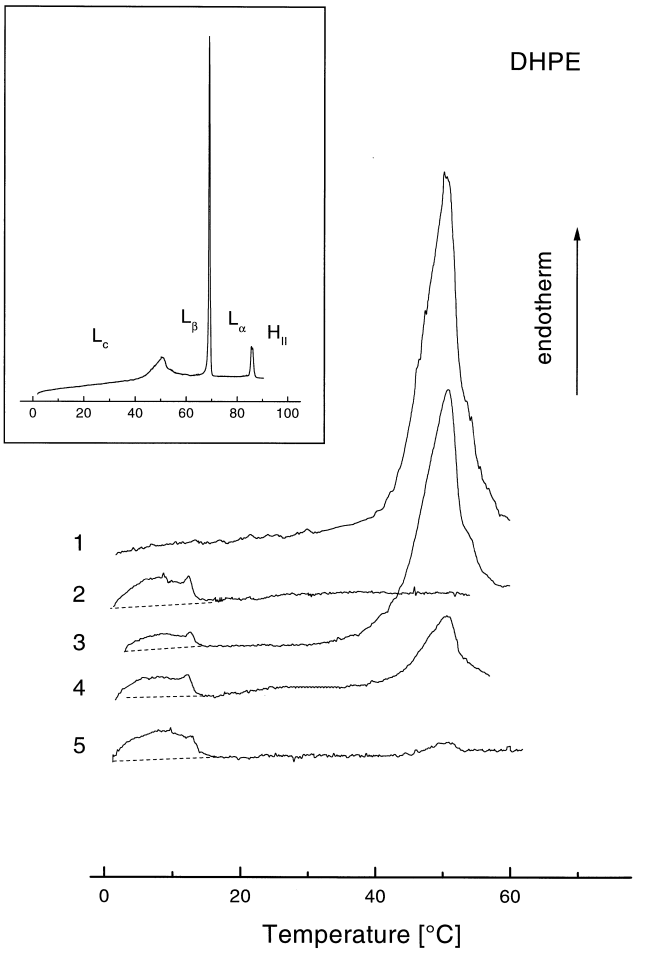

Fig. 4. DSC heating thermograms (low-temperature portions) of hydrated DHPE dispersion recorded after different thermal prehistory: 1, first heating after low-temperature sample preparation; 2, immediate second heating after cooling to 0°C; 3, second heating after cooling to −18°C for 30 min and subsequent 15 h storage at 3°C; 4, second heating after cooling to −18°C for 30 min and subsequent 3 h storage at 3°C; 5, second heating after 60 h incubation at 3°C. Inset: full-scale thermogram of the initial heating of a DHPE sample prepared at low temperature. Heating rate 0.5°C/min.

conversion, the peak at 10°C does not change in temperature but only decreases in enthalpy, in parallel to the growth of the $L_c \rightarrow L_\beta$ peak at 50°C. The applied incubation protocols did not invariably induce the lipid samples to exhibit the extents of recovery of the L_c phase demonstrated on Fig. 4. With some samples, the crystallisation rate was much lower. Poor reproducibility of the crystallisation kinetics has been reported for dilauroyl PE as well [23]. However, the characteristics of the $L_{R1} \rightarrow L_\beta$ transition of

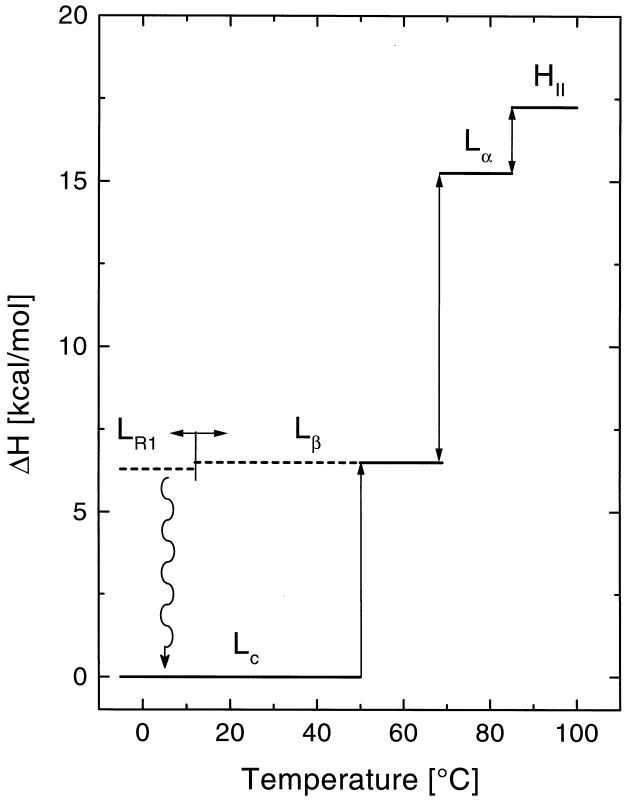

Fig. 5. Summary of transition pathways, temperatures and enthalpies for fully hydrated DHPE. The wavy line represents isothermal relaxation of the L_{R1} phase into L_c phase.

DHPE were invariant. Similar low-temperature, low-enthalpy peaks were also observed for DHPE dispersions in up to 2 M sucrose solutions. One may conclude on basis of the calorimetric data that no other thermodynamically distinct states intervene in the relaxation of L_{R1} into L_c phase. They also show that the L_{R1} phase of DHPE can only be entered by cooling of the gel L_β phase. Once formed, the L_c phase of this lipid converts directly into L_β phase at the temperature of 50°C, skipping the L_{R1} phase.

The L_{R1} phase seems to be an obligatory prerequisite for the formation of the equilibrium L_c phase in DHPE. Upon incubation of the gel L_β phase at room temperature (about 20°C), above the L_{R1}–L_β transition temperature, and without preceding cooling below the last temperature, no formation of an L_c phase has been noticed even after 1 month, according to both X-ray diffraction and microcalorimetry. It thus appears that a direct conversion of the metastable gel L_β phase into L_c phase, although thermodynamically not forbidden, is kinetically strongly hindered, and that an $L_\beta \rightarrow L_{R1} \rightarrow L_c$ conversion is the only observable pathway for formation of an L_c phase. A summary of the transition pathways, temperatures and enthalpies for hydrated DHPE is given in Fig. 5.

The low-temperature phase behaviour of DHPE dispersions appears to resemble the thermotropic polymorphism observed for long-chain normal alkanes. The latter compounds are known to form at least five different solid phases, from R_I to R_V, one or more of which may appear as intermediate phases in temperature scans from the fluid phase, which is stable at high temperature, into the crystalline phase, which is stable at low temperature [17]. For the lack of long-range order in the rotational degree of freedom about the long axis of the alkane molecules, these intermediate phases have been termed 'rotator' (R) phases. With respect to hydrocarbon chain arrangements, they differ from each other by the chain tilt with respect to the layer normal and by the hexagonal or orthorhombic chain arrangements. Following such analogy, the L_β and L_{R1} phases of DHPE appear to correspond to the R_{II} and R_I rotator phases. In the latter two, untilted alkane molecules are packed on hexagonal and orthorhombic lattice, respectively. Whenever present, these phases appear in the sequence fluid $\rightarrow R_{II} \rightarrow R_I \rightarrow$ crystal phase [17], similarly to the sequence $L_\alpha \rightarrow L_\beta \rightarrow L_{R1} \rightarrow L_c$ found for DHPE. Furthermore, examples have been provided where the metastable R_I alkane phase can be only entered by cooling, and not by heating of the crystalline phase, similarly to the L_{R1} phase of DHPE (Fig. 5). In view of these similarities, it appears that chain–chain interactions play dominant role for the $L_\beta \leftrightarrow L_{R1}$ transition of DHPE. To emphasise the parallelism with the R_I alkane phase, we have adopted the notation L_{R1} for the described here ordered low-temperature phase of DHPE.

In conclusion, the facile, reversible transformation of the DHPE L_β phase into L_{R1} phase requires no low-temperature incubation and initiates immediately upon cooling to 12°C. It includes no change of the lamellar repeat distance but only a hydrocarbon chain reorganisation from hexagonal to orthorhombic packing. This transition is associated with a small ($\sim$2 μl/g) decrease of the lipid partial specific volume and an enthalpy change of about 0.2 kcal/mol. The formation of the L_c phase in DHPE dis-

persions appears to proceed from only within the L_{R1} phase, and not by means of direct relaxation of L_β into L_c phase. Earlier X-ray studies have demonstrated the existence of similar ordered phases in fully hydrated PEs and dispersions of phosphatidic acids in 1M NaCl solutions [3,4]. The observed decrease of the $L_{R1} \rightarrow L_\beta$ calorimetric peak with increase of the $L_c \rightarrow L_\beta$ endotherm (subtransition) upon low-temperature storage of DHPE resembles the picture documented for the low-temperature phase evolution in DPPC [5,6]. It has been established that aqueous DPPC dispersions, upon cooling of their gel phase, undergo a rapidly reversible low-enthalpy transition to an intermediate metastable state (SGII, 'sub-subgel', according to [5]), from which the formation of the equilibrium L_c phase can only take place upon subsequent incubation [5–7]. Similar reversible low-temperature, low-enthalpy transitions were recorded by DSC also in dimyristoyl PC and distearoyl PC dispersions [7]. In another study, we observed a reversible splitting (the Y-transition) of the gel phase WAX reflection in DHPE dispersed in concentrated sucrose solutions [15]. Thus, the occurrence of ordered metastable phases upon cooling of the lipid L_β phase, as precursors in the formation of an L_c phase, appears to be a general feature for a variety of lipid-water systems.

Acknowledgements

R.K. and B.T. acknowledge EU support for the work at EMBL Hamburg and support from the Bulgarian National Science Foundation.

References

[1] Lipid Thermodynamic Database, LIPIDAT, http://www.LIPIDAT.chemistry.ohio-state.edu
[2] R. Koynova, J. Brankov, B. Tenchov, Eur. Biophys. J. 25 (1997) 261–275.
[3] K. Harlos, Biochim. Biophys. Acta 511 (1978) 348–355.
[4] K. Harlos, H. Eibl, Biochemistry 20 (1981) 2888–2892.
[5] J.L. Slater, C. Huang, Biophys. J. 52 (1987) 667–670.
[6] M. Kodama, H. Hashigami, S. Seki, J. Colloid Interface Sci. 117 (1987) 497–504.
[7] R. Koynova, B.G. Tenchov, S. Todinova, P.J. Quinn, Biophys. J. 68 (1995) 2370–2375.
[8] M. Rappolt, G. Rapp, Ber. Bunsenges. Phys. Chem. 100 (1996) 1153–1162.
[9] J. Hendrix, M.H.J. Koch, J. Bordas, Appl. Cryst. 12 (1979) 467–472.
[10] G. Rapp, A. Gabriel, M. Dosiere, M.H.J. Koch, Nucl. Instrum. Meth. Phys. Res. A 357 (1995) 178–182.
[11] C. Boulin, R. Kempf, M.H.J. Koch, S.M. McLaughlin, Nucl. Instrum. Methods A249 (1986) 399–407.
[12] R.C. Weast (Ed.), CRC Handbook of Chemistry and Physics, 66th ed., CRC Press, Boca Raton, FL, 1985–86.
[13] A. Tardieu, V. Luzzati, F.C. Reman, J. Mol. Biol. 75 (1973) 711–733.
[14] T.J. McIntosh, Biophys. J. 29 (1980) 237–246.
[15] B. Tenchov, M. Rappolt, R. Koynova, G. Rapp, Biochim. Biophys. Acta 1285 (1996) 109–122.
[16] D.M. Small, Handbook of Lipid Research, vol. 4, The Physical Chemistry of Lipids, Plenum Press, New York, 1986.
[17] E.B. Sirota, H.E. King Jr., D.M. Singer, H.H. Shao, J. Chem. Phys. 98 (1993) 5809–5824.
[18] J.M. Seddon, J.L. Hogan, N.A. Warrender, E. Pebay-Peyroula, Progr. Colloid Polym. Sci. 81 (1990) 189–197.
[19] M. Caffrey, Biochemistry 24 (1985) 4826–4844.
[20] F.S. Hing, P.R. Maulik, G.G. Shipley, Biochemistry 30 (1991) 9007–9015.
[21] J.F. Nagle, M.C. Wiener, Biochim. Biophys. Acta 942 (1988) 1–10.
[22] R. Koynova, M. Caffrey, Chem. Phys. Lipids 69 (1994) 1–34.
[23] J. Seddon, K. Harlos, D. Marsh, J. Biol. Chem. 258 (1983) 3850–3854.